Enhancement of London Dispersion in Frustrated Lewis Pairs: Towards a Crystalline Encounter Complex

Flip Holtrop[◇a]
Christoph Helling[◇a]
Martin Lutz[b]
Nicolaas P. van Leest[a]
Bas de Bruin[a] [ORCID]
J. Chris Slootweg*[a] [ORCID]

[a] Van 't Hoff Institute for Molecular Sciences, University of Amsterdam, PO Box 94157, 1090 GD Amsterdam, The Netherlands
j.c.slootweg@uva.nl
[b] Structural Biochemistry, Bijvoet Centre for Biomolecular Research, Utrecht University, Universiteitsweg 99, 3584 CG Utrecht, The Netherlands
[◇] These authors contributed equally
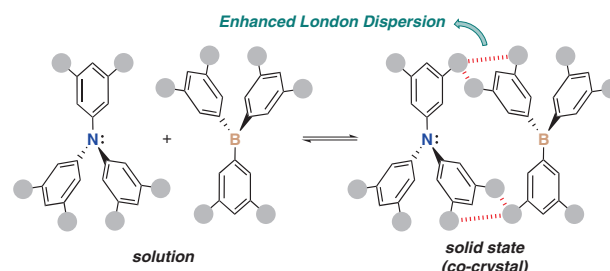
Enhanced London Dispersion

solution ⇌ solid state (co-crystal)

Abstract The encounter complex, *i.e.*, the pre-organized assembly consisting of a Lewis acid and a Lewis base, is a fundamental concept in frustrated Lewis pair (FLP) chemistry. However, this donor–acceptor complex is challenging to study due to its transient nature. Here, we present a combined theoretical and experimental investigation on the potential isolation of an encounter complex enabled by enhancement of London dispersion forces between a sterically encumbered Lewis acid and base pair. Guided by computational analyses, the FLP originating from the bulky triarylamine $N(3,5-tBu_2C_6H_3)_3$ and the novel triarylborane $B(3,5-tBu_2C_6H_3)_3$ was investigated, leading to the isolation of a 1:1 co-crystal of both FLP components.

Key words frustrated Lewis pairs, encounter complex, London dispersion forces, Lewis acid, Lewis base

Since their discovery in 2006,[1] the potential of frustrated Lewis pairs (FLPs) for the metal-free activation of small molecules, such as H_2 and CO_2, has been extensively showcased.[2] However, particularly for substrates like H_2 that only weakly interact with the individual FLP components, the activation mechanism still remains ambiguous. This is due to the weak interactions between the Lewis acid and Lewis base in intermolecular FLPs resulting in highly fluxional structures of low concentrations in solution, which are thus challenging to study and characterize by spectroscopic methods.[3] A number of computational investigations sug-

gested the pre-organization of the FLP components to form an encounter complex, in which the interaction is governed by London dispersion forces between the bulky substituents (Figure 1a).[4] The first experimental evidence for such association was provided through $^{19}F,^{1}H$ HOESY NMR studies by Rocchigiani and co-workers revealing intermolecular H–F interactions in concentrated solutions of archetypical FLPs $R_3P/B(C_6F_5)_3$ (R = Mes, tBu).[5] Further evidence of the encounter complex in solution was provided by UV/Vis and transient absorption spectroscopy. The detection of charge-transfer bands of FLPs $R_3P/B(C_6F_5)_3$ established the equivalence of encounter complexes with electron donor–acceptor (EDA) complexes and allowed for the observation of radical ion pairs resulting from photoinduced single-electron transfer (SET) between the associated Lewis base and Lewis acid by EPR spectroscopy.[6] However, to date, solid-state
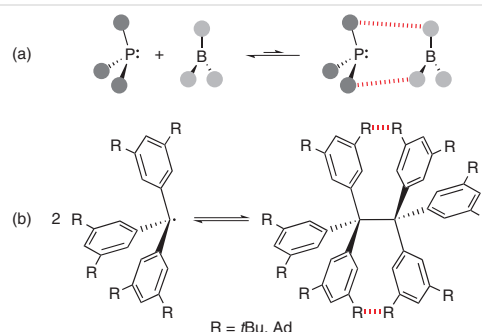

Figure 1 (a) Reversible association of the encounter complex in archetypical FLP systems. (b) London dispersion facilitated reversible dimerization of all-*meta*-substituted triphenylmethyl radicals.[8] Red-dashed lines indicate London dispersion interactions.

1123

Synlett   F. Holtrop et al.   THIEME OPEN ACCESS   Cluster

structures of intermolecular FLPs potentially revealing key information on the FLP pre-organization have not yet been crystallographically characterized.[7]
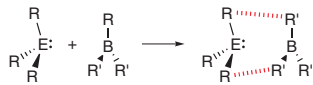
Schreiner and co-workers demonstrated that the reversible head-to-head association of bulky, all-*meta*-substituted triphenylmethyl radicals to the corresponding hexaphenylethane derivatives can be attributed to attractive London dispersion forces between the *meta* substituents and that the extent of stabilization of the dimeric structure can be tuned depending on the quality of the dispersion energy donor (Figure 1b).[8]

In line with our general interest in the reactivity and reaction mechanisms of FLP systems,[6,9] we envisioned the utilization of London dispersion stabilization to increase the attraction between the Lewis acid and the Lewis base of an FLP, enhance the pre-organization of the FLP components, which should increase its concentration in solution, ultimately to enable the isolation and (solid-state) characterization of the encounter complex. For this, we computationally investigated the stability of potential encounter complexes containing all-*meta*-substituted triarylamines/-phosphines and triarylboranes and studied promising combinations experimentally.

Employing an approach analogous to the London dispersion facilitated formation of all-*meta*-substituted hexaphenylethanes, we included triarylamines N(3,5-*t*Bu$_2$C$_6$H$_3$)$_3$ and N(3,5-Ph$_2$C$_6$H$_3$)$_3$ as well as triarylphosphine P(3,5-*t*Bu$_2$C$_6$H$_3$)$_3$ as the Lewis basic component of potential FLPs in our investigation. For the Lewis acidic counterpart all-*meta*-substituted triarylboranes B(3,5-*t*Bu$_2$C$_6$H$_3$)$_3$, B(3,5-Ph$_2$C$_6$H$_3$)$_3$, and B(3,5-(CF$_3$)$_2$C$_6$H$_3$)$_3$ as well as B(C$_6$F$_5$)$_3$ were selected. Moreover, archetypical FLP combinations R$_3$P/B(C$_6$F$_5$)$_3$ (R = Mes, *t*Bu) were included for comparison. For the computational analysis, initially, the structures of encounter complexes for the different combinations of Lewis acids and Lewis bases were optimized at the ωB97XD/6-311+G(d,p)//ωB97XD/6-31G(d) level of theory, and the formation energies were determined (Table 1).

Inspection of the obtained formation energies of encounter complexes obtained from all-*meta*-substituted triarylamines as well as phosphines together with B(C$_6$F$_5$)$_3$ already revealed a significantly increased stability (–20.32 to –33.31 kcal mol^{-1}) compared to the encounter complexes arising from R$_3$P/B(C$_6$F$_5$)$_3$ (R = Mes –13.90 kcal mol^{-1}, *t*Bu –13.87 kcal mol^{-1}). Substitution of B(C$_6$F$_5$)$_3$ leads to a further increase in stability of the encounter complex, following the order B(C$_6$F$_5$)$_3$ < B(3,5-(CF$_3$)$_2$C$_6$H$_3$)$_3$ < B(3,5-*t*Bu$_2$C$_6$H$_3$)$_3$ < B(3,5-Ph$_2$C$_6$H$_3$)$_3$. However, it must be noted that the examined P(3,5-*t*Bu$_2$C$_6$H$_3$)$_3$/BR$_3$ (R = C$_6$F$_5$, 3,5-(CF$_3$)$_2$C$_6$H$_3$, 3,5-*t*Bu$_2$C$_6$H$_3$) combinations converged to the corresponding classical P–B-bonded Lewis adducts as a result of the longer P–B and P–C bond lengths, effectively reducing the steric bulk of the phosphine. Therefore, the systems containing P(3,5-*t*Bu$_2$C$_6$H$_3$)$_3$ as the Lewis base are not suitable for fur-
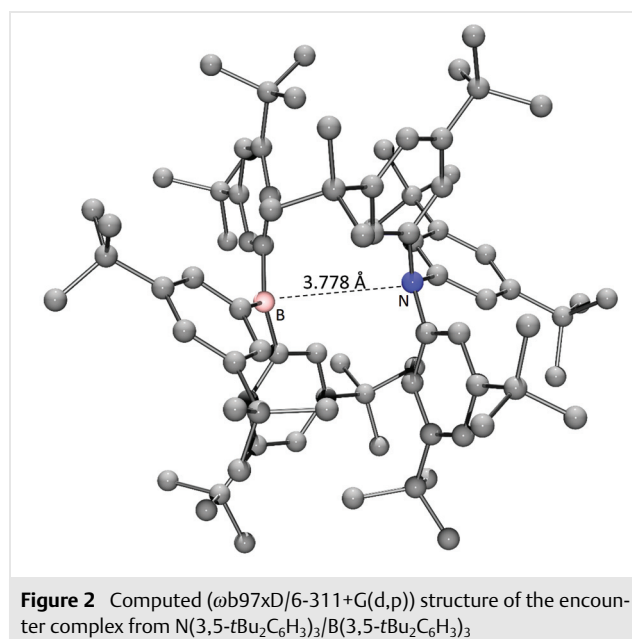
Table 1 Encounter Complex-Formation Energies (kcal mol^{-1})[a]

Lewis base	Lewis acid	ΔE_{tot}	ΔE_{Disp}
PMes$_3$	B(C$_6$F$_5$)$_3$	–13.90	– 7.95
P*t*Bu$_3$	B(C$_6$F$_5$)$_3$	–13.87	– 5.60
N(3,5-*t*Bu$_2$C$_6$H$_3$)$_3$	B(3,5-*t*Bu$_2$C$_6$H$_3$)$_3$	–39.93	–25.33
	B(3,5-Ph$_2$C$_6$H$_3$)$_3$	–43.73	–27.84
	B(3,5-(CF$_3$)$_2$C$_6$H$_3$)$_3$	–35.01	–20.71
	B(C$_6$F$_5$)$_3$	–20.32	–13.00
N(3,5-Ph$_2$C$_6$H$_3$)$_3$	B(3,5-*t*Bu$_2$C$_6$H$_3$)$_3$	–46.60	–28.17
	B(3,5-Ph$_2$C$_6$H$_3$)$_3$	–54.20	–32.49
	B(3,5-(CF$_3$)$_2$C$_6$H$_3$)$_3$	–40.85	–21.56
	B(C$_6$F$_5$)$_3$	–27.68	–15.66
P(3,5-*t*Bu$_2$C$_6$H$_3$)$_3$	B(3,5-*t*Bu$_2$C$_6$H$_3$)$_3$	–51.58	–26.80
	B(3,5-(CF$_3$)$_2$C$_6$H$_3$)$_3$	–53.80	–21.30
	B(C$_6$F$_5$)$_3$	–33.31	–13.55

[a] Calculated at the ωB97xD/6-311+G(d,p) level of theory.

ther experimental investigations of encounter complexes. In contrast, the optimized structures containing the triarylamines show no considerable amount of N–B interactions as assessed by the essentially planar B centers and the large N–B distances (3.693–4.502 Å). For instance, in case of N(3,5-*t*Bu$_2$C$_6$H$_3$)$_3$/B(3,5-*t*Bu$_2$C$_6$H$_3$)$_3$ a N–B separation of 3.778 Å was obtained (Figure 2), which is in sharp contrast

Figure 2 Computed (ωb97xD/6-311+G(d,p)) structure of the encounter complex from N(3,5-*t*Bu$_2$C$_6$H$_3$)$_3$/B(3,5-*t*Bu$_2$C$_6$H$_3$)$_3$

1124

Syn*lett*   F. Holtrop et al.   THIEME OPEN ACCESS   **Cluster**

to the weakly bound classical Lewis pair lutidine/B(C$_6$F$_5$)$_3$ that features a N–B bond length of 1.661(2) Å, as determined single-crystal X-ray crystallography.[10]

Having established the increased stability of the encounter complexes with Lewis acids and Lewis bases containing dispersion energy donors, we aimed at a closer inspection and quantification of the London dispersion forces between the Lewis acidic and Lewis basic fragments since the initial computations only account for the total dispersion within the system, *i.e.*, the intermolecular and intramolecular dispersion combined. Therefore, we performed energy decomposition and fragment analyses (ADF; M06-2X-D3/TZ2P) disclosing the interaction energies between the FLP components (Table 2). Again, the FLPs R$_3$P/B(C$_6$F$_5$)$_3$ (R = Mes, *t*Bu) were included as reference.

Table 2 Calculated Interaction Energies (kcal mol^{-1}) between Lewis Acid and Lewis Base in the Encounter Complexes of Studied FLPs[a]

Lewis base	Lewis acid	$E_{int,tot}$	$E_{int,Disp}$
PMes$_3$	B(C$_6$F$_5$)$_3$	–13.17	– 3.89
P*t*Bu$_3$	B(C$_6$F$_5$)$_3$	–13.90	– 3.14
N(3,5-*t*Bu$_2$C$_6$H$_3$)$_3$	B(3,5-*t*Bu$_2$C$_6$H$_3$)$_3$	–40.44	–11.45
	B(3,5-Ph$_2$C$_6$H$_3$)$_3$	–40.76	–11.68
	B(3,5-(CF$_3$)$_2$C$_6$H$_3$)$_3$	–32.59	– 8.52
	B(C$_6$F$_5$)$_3$	–20.89	– 6.31
N(3,5-Ph$_2$C$_6$H$_3$)$_3$	B(3,5-*t*Bu$_2$C$_6$H$_3$)$_3$	–41.00	–11.79
	B(3,5-Ph$_2$C$_6$H$_3$)$_3$	–47.32	–11.83
	B(3,5-(CF$_3$)$_2$C$_6$H$_3$)$_3$	–34.82	– 8.19
	B(C$_6$F$_5$)$_3$	–26.79	– 6.42

[a] Calculated at the M06-2X-D3/TZ2P level of theory.

Exchanging the phosphine of FLP systems R$_3$P/B(C$_6$F$_5$)$_3$ (R = Mes –3.89 kcal mol^{-1}, *t*Bu –3.14 kcal mol^{-1}) for all-*meta*-substituted amines N(3,5-*t*Bu$_2$C$_6$H$_3$)$_3$ (–6.31 kcal mol^{-1}) and N(3,5-Ph$_2$C$_6$H$_3$)$_3$ (–6.42 kcal mol^{-1}) leads to a doubling of the amount of London dispersion stabilization between the FLP components in the encounter complex. Altering the Lewis acid to B(3,5-(CF$_3$)$_2$C$_6$H$_3$)$_3$ (–8.52 (*t*Bu), –8.19 (Ph) kcal mol^{-1}) only shows a marginal increase in dispersion interactions compared to B(C$_6$F$_5$)$_3$, whereas employing all-*meta*-substituted boranes B(3,5-*t*Bu$_2$C$_6$H$_3$)$_3$ (–11.45 (*t*Bu), –11.68 (Ph) kcal mol^{-1}) and B(3,5-Ph$_2$C$_6$H$_3$)$_3$ (–11.79 (*t*Bu), –11.83 (Ph) kcal mol^{-1}) effects a further doubling of the amount of London dispersion stabilization. The calculations moreover revealed no significant differences in the dispersion energy for the all-*meta*-Ph and all-*meta*-*t*Bu systems making these combinations equally promising candidates for experimental investigations. By installing dispersion energy donors on both Lewis acid and Lewis base, a total increase in the dispersion stabilization of approximately 8 kcal mol^{-1} was achieved according to the gas-

phase computations. Recent studies demonstrated that dispersion interactions are attenuated in solution to a large extent (about 70%),[11] which results in an expected increased stabilization of the encounter complex comprising all-*meta*-substituted triarylamines and boranes in solution of approximately 2.5 kcal mol^{-1} via interfragment dispersion interactions. This stabilization of the encounter complex is still significant and could lead to a shift in the equilibrium and an increased encounter complex concentration in solution.

Since the interfragment interactions in the N(3,5-R$_2$C$_6$H$_3$)$_3$/B(3,5-R$_2$C$_6$H$_3$)$_3$ systems mostly correspond to London dispersion forces with negligible contributions from the N–B interaction, we furthermore calculated the formation energies of the homodimers N(3,5-R$_2$C$_6$H$_3$)$_3$/N(3,5-R$_2$C$_6$H$_3$)$_3$ and B(3,5-R$_2$C$_6$H$_3$)$_3$/B(3,5-R$_2$C$_6$H$_3$)$_3$ and examined the fragment interactions by energy decomposition analysis (Table 3).

Table 3 Homodimer Formation[a] and Fragment Interaction[b] Energies (kcal mol^{-1})

R	Complex	ΔE_{tot}	ΔE_{Disp}	$E_{int,tot}$	$E_{int,Disp}$
3,5-*t*Bu$_2$C$_6$H$_3$	NR$_3$/BR$_3$	–39.93	–25.33	–40.44	–11.45
	NR$_3$/NR$_3$	–41.03	–26.09	–39.57	–11.55
	BR$_3$/BR$_3$	–37.54	–23.61	–37.99	–11.31
3,5-Ph$_2$C$_6$H$_3$	NR$_3$/BR$_3$	–54.20	–32.49	–47.32	–11.83
	NR$_3$/NR$_3$	–54.20	–31.14	–45.73	–11.91
	BR$_3$/BR$_3$	–54.00	–33.54	–45.60	–11.90

[a] Calculated at the ωB97xD/6-311+G(d,p) level of theory.
[b] Calculated at the M06-2X-D3/TZ2P level of theory.

The computational analysis revealed similar formation and dispersion interaction energies for the amine–amine (–11.55 (*t*Bu), –11.91 (Ph) kcal mol^{-1}) and borane–borane (–11.31 (*t*Bu), –11.90 (Ph) kcal mol^{-1}) dimers as for the amine–borane systems, suggesting that amine–borane encounter complex and homodimer formation are equally favored.

As a result of the computational analysis, we investigated combinations consisting of all-*meta*-*t*Bu-substituted triarylamine N(3,5-*t*Bu$_2$C$_6$H$_3$)$_3$ as the Lewis base and triarylboranes B(3,5-(CF$_3$)$_2$C$_6$H$_3$)$_3$ and B(3,5-*t*Bu$_2$C$_6$H$_3$)$_3$ as Lewis acids in the subsequent experimental investigation.[12] Amine N(3,5-*t*Bu$_2$C$_6$H$_3$)$_3$ was synthesized according to a literature procedure.[13] For purposes of comparison, single crystals of N(3,5-*t*Bu$_2$C$_6$H$_3$)$_3$ were grown from pentane at –30 °C and the solid-state structure was determined by single-crystal X-ray structure analysis. The crystal structure of the current pentane solvate is isostructural with the toluene solvate of the corresponding hydrocarbon.[14] The central nitrogen atom and one phenyl ring are located on a twofold axis. The nitrogen geometry is planar with an angle sum of

360.0(3)° and N–C distances of 1.430(3) Å and 1.424(2) Å. The aryl groups are arranged propeller-like with C–N–C–C torsion angles of –39.37(15)° and –35.3(2)°. Two of the *t*Bu groups were refined with a disorder model (Figure 3). The crystal structure contains no intermolecular N···N distances shorter than 10 Å.
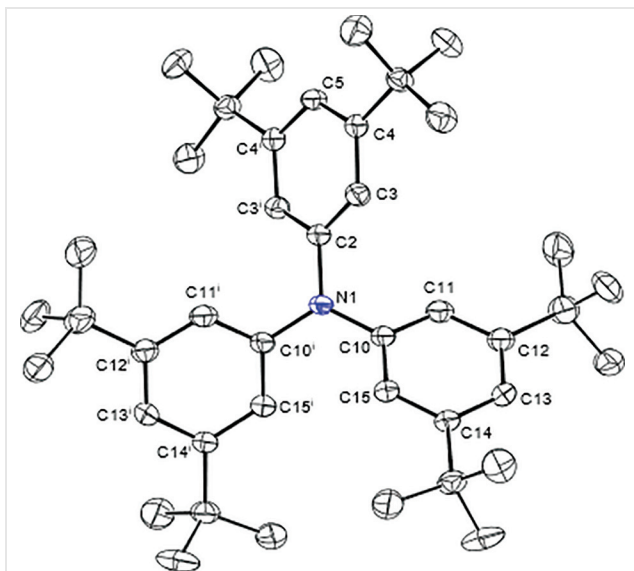

Figure 3 Displacement ellipsoid plot of N(3,5-*t*Bu$_2$C$_6$H$_3$)$_3$ in the crystal (50% probability level). Only the major disorder component is shown. Hydrogen atoms and pentane solvent molecule are omitted for clarity. Symmetry code *i*: -x, y, ½-z.

B(3,5-(CF$_3$)$_2$C$_6$H$_3$)$_3$ was obtained following a literature procedure,[15] whereas B(3,5-*t*Bu$_2$C$_6$H$_3$)$_3$ could not be obtained in an analogous manner due to the formation of complex product mixtures from which the borane could not be isolated. However, the synthesis of B(3,5-*t*Bu$_2$C$_6$H$_3$)$_3$ was achieved *via* a modified synthetic route for BPh$_3$ developed by Lammertsma et al.[16] First, Na[B(3,5-*t*Bu$_2$C$_6$H$_3$)$_4$] (^{11}B NMR: δ = –4.72) was synthesized by reaction of NaBF$_4$ with four equivalents of Li(3,5-*t*Bu$_2$C$_6$H$_3$). Subsequently, [Me$_3$NH][B(3,5-*t*Bu$_2$C$_6$H$_3$)$_4$] was generated *in situ* by cation exchange using [Me$_3$NH]Cl, which spontaneously eliminates NMe$_3$ and 1,3-*t*Bu$_2$C$_6$H$_4$ with formation of B(3,5-*t*Bu$_2$C$_6$H$_3$)$_3$ upon treatment with THF.[17] It was found, though, that B(3,5-*t*Bu$_2$C$_6$H$_3$)$_3$ is highly susceptible towards decomposition upon workup of the reaction mixture. Isolation of B(3,5-*t*Bu$_2$C$_6$H$_3$)$_3$ was achieved by addition of 2,2,6,6-tetramethylpiperidine to the THF solution to scavenge any residual protons, removal of volatiles, and extraction into Et$_2$O, from which colorless X-ray quality single crystals were obtained after storage at –30 °C (Scheme 1).[18]

Borane B(3,5-*t*Bu$_2$C$_6$H$_3$)$_3$ features the expected signals for the aryl groups in its ^{1}H and ^{13}C{^{1}H} NMR spectra. The ^{11}B NMR spectrum exhibits a broad resonance at 68.4 ppm, comparable to that of BPh$_3$ (67.8 ppm).[16] The molecular
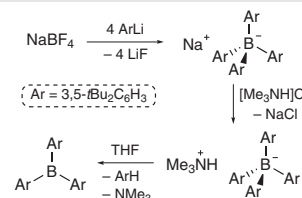
Scheme 1 Synthesis of B(3,5-*t*Bu$_2$C$_6$H$_3$)$_3$

structure of B(3,5-*t*Bu$_2$C$_6$H$_3$)$_3$ determined by X-ray crystal-structure determination features the expected trigonal-planar coordination geometry at B with an angle sum of 360.1(4)°. Here, the boron atom is on a general position without symmetry. The propeller-like arrangement of the aryl substituents can be seen in the C–B–C–C torsion angles of –31.4(4)°, –32.6(4), and –34.7(4)°. The B–C bond lengths are in the range of 1.558(4)–1.570(4) Å (Figure 4). The overall geometry is highly similar to that of N(3,5-*t*Bu$_2$C$_6$H$_3$)$_3$. Again, there are no intermolecular B···B distances shorter than 10 Å.
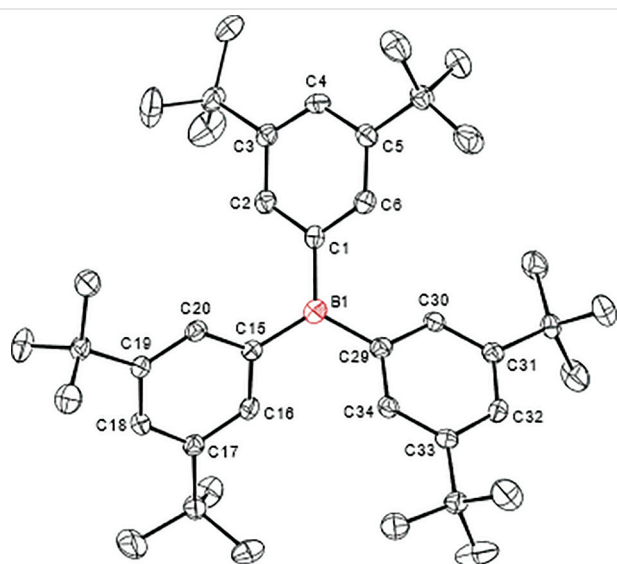

Figure 4 Displacement ellipsoid plot of B(3,5-*t*Bu$_2$C$_6$H$_3$)$_3$ in the crystal (50% probability level). Only the major disorder component is shown. Hydrogen atoms and diethyl ether solvent molecule are omitted for clarity.

With the Lewis acids and Lewis base in hand, encounter complex formation was investigated. Mixing solutions of N(3,5-*t*Bu$_2$C$_6$H$_3$)$_3$ and B(3,5-(CF$_3$)$_2$C$_6$H$_3$)$_3$ in toluene or dichloromethane initially yielded a pale yellow solution which gradually turned dark blue over the course of several hours. As the dark blue color is characteristic of triarylamine radical cations, EPR analysis was conducted. The X-band EPR spectrum (Figure 5) of this solution revealed a

signal featuring a multitude of hyperfine coupling interactions characteristic for an organic radical in a doublet spin system, indicating formation of $^{+\bullet}$N(3,5-tBu$_2$C$_6$H$_3$)$_3$.
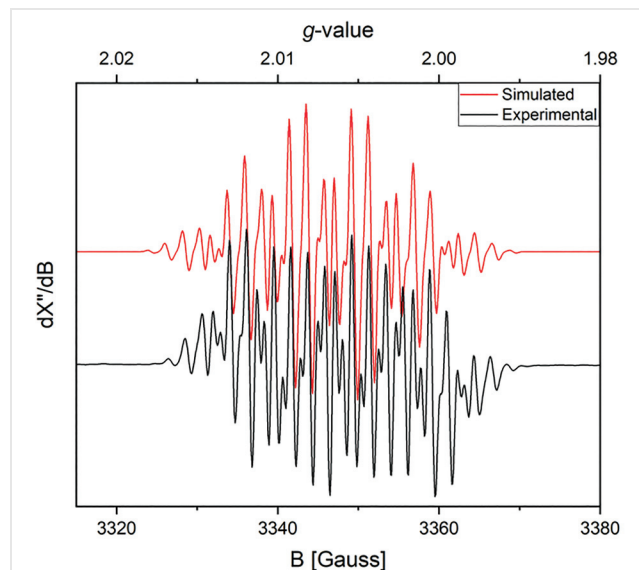
Figure 5 Simulated (red) and experimental (black) X-band EPR spectrum of $^{+\bullet}$N(3,5-tBu$_2$C$_6$H$_3$)$_3$ in dichloromethane (capillary) at room temperature. Experimental parameters; microwave frequency 9.388019 GHz, power 0.7962 mW, modulation amplitude; 1.000 G. Simulation parameters; $S = \frac{1}{2}$, $g_{iso} = 2.0042$, $A^{14N}_{iso} = 21.5777$ MHz, $6 \times A^{1H\text{-}ortho}_{iso} = -6.0593$, $3 \times A^{1H\text{-}para}_{iso} = -15.4771$, lw = 0.067165.

Satisfactory simulation of the experimental spectrum was achieved with $g_{iso} = 2.0042$ and inclusion of hyperfine coupling interactions with nitrogen ($A^{14N}_{iso} = 21.58$ MHz), six equivalent protons (*ortho*-protons on the aryl moieties of the amine; $A^{1H\text{-}ortho}_{iso} = -6.06$ MHz), and another three equivalent protons (*para* protons on the aryl moieties of the amine; $A^{1H\text{-}para}_{iso} = -15.48$ MHz) consistent with the presence of $^{+\bullet}$N(3,5-tBu$_2$C$_6$H$_3$)$_3$. Moreover, the calculated EPR parameters for $^{+\bullet}$N(3,5-tBu$_2$C$_6$H$_3$)$_3$ by DFT ($g_{iso} = 2.0030$, $A^{14N}_{iso} = 21.20$ MHz, $A^{1H\text{-}ortho}_{iso} = -6.18$ MHz, $A^{1H\text{-}para}_{iso} = -9.18$ MHz) are in reasonable agreement with the simulated data. Further support was obtained by independent generation of $^{+\bullet}$N(3,5-tBu$_2$C$_6$H$_3$)$_3$ via the oxidation of N(3,5-tBu$_2$C$_6$H$_3$)$_3$ with Cu(ClO$_4$)$_2$[19] and simulation of the obtained spectra (Figures S9, S10), which can be achieved with the same hyperfine coupling constants and a g_{iso} value of 2.0028. The formation of $^{+\bullet}$N(3,5-tBu$_2$C$_6$H$_3$)$_3$ in the reaction of N(3,5-tBu$_2$C$_6$H$_3$)$_3$ and B(3,5-(CF$_3$)$_2$C$_6$H$_3$)$_3$ is in line with previous reports on the one-electron oxidation of triarylamines by B(C$_6$F$_5$)$_3$[20] and our investigation on photoinduced SET in FLP systems,[6] driven by rapid decomposition of the corresponding triarylborane radical anion *via* solvolytic pathways.[21] This photolability is expected to complicate characterization and isolation of the corresponding encounter complex. Crystallization of an encounter complex with exclusion of light proved unsuccessful. Therefore, we focused on B(3,5-tBu$_2$C$_6$H$_3$)$_3$ as Lewis acid. The decreased Lewis acidity and electron affinity of B(3,5-tBu$_2$C$_6$H$_3$)$_3$ leads to a large energy gap for the excitation of the charge-transfer complex to the corresponding radicals ($\Delta E = 4.26$ eV (291 nm); Table S1) preventing visible-light-induced SET.

Mixing solutions of N(3,5-tBu$_2$C$_6$H$_3$)$_3$ and B(3,5-tBu$_2$C$_6$H$_3$)$_3$ in toluene produced a colorless solution and ^{1}H NMR spectroscopic analysis only showed the presence of the starting materials as typically observed for FLP systems.[22] Attempts to observe a potential pre-organization of the FLP in solution by ^{1}H,^{1}H NOESY NMR studies revealed no through-space correlations between the protons of the Lewis acid and the Lewis base. This could be a result of the limited solubility of the FLP and its components precluding analysis of highly concentrated solutions as used by Rocchigiani and co-workers.[5] Moreover, homodimer association could further reduce the effective concentration of Lewis acid–Lewis base couples in solution. However, due the limited solubility, crystallization of colorless crystals was achieved from both toluene and n-pentane solutions.[23] The X-ray crystal-structure determination of the N(3,5-tBu$_2$C$_6$H$_3$)$_3$/B(3,5-tBu$_2$C$_6$H$_3$)$_3$ crystals showed that these crystals are isostructural to the pentane solvate of N(3,5-tBu$_2$C$_6$H$_3$)$_3$ described above (see the Supporting Information). In addition to sharp Bragg reflections these crystals showed diffuse peaks for reflections with ℓ = *odd* (Figure S15). Due to similar X-ray scattering factors of nitrogen and boron, it was not possible to assign these centers unambiguously and thus resolve substitutional disorder of the central atom, which is why the occupancy was set to $\frac{1}{2}$ for both elements. The formation of a co-crystal is supported by NMR spectroscopic analysis of the isolated crystals showing a 1:1 mixture of N(3,5-tBu$_2$C$_6$H$_3$)$_3$ and B(3,5-tBu$_2$C$_6$H$_3$)$_3$ (Figures S11, S12), which proves the presence of both components in the crystal lattice. Moreover, the IR spectrum of the isolated crystals (Figure S13) exhibits features found in the IR spectra of both separate components (Figures S1, S8), while the melting point (224 °C) lies between those of N(3,5-tBu$_2$C$_6$H$_3$)$_3$ (201 °C) and B(3,5-tBu$_2$C$_6$H$_3$)$_3$ (255 °C). The random stacking of both components in the crystal lattice yielding an overall 1:1 ratio of Lewis acid and Lewis base most likely results from the almost identical shapes of N(3,5-tBu$_2$C$_6$H$_3$)$_3$ and B(3,5-tBu$_2$C$_6$H$_3$)$_3$ and the computed similar hetero- and homofragment dispersion interaction energies between the components of the FLP (Table 3) resulting in no significant driving force towards an alternating pattern. Still, this result emphasizes the importance of London dispersion forces in FLP chemistry and the possibility of crystallizing the encounter complex.

On the basis of computational analyses, which showed that the London dispersion forces between the components of FLP systems can be significantly enhanced by judicious choice of the substituents at the Lewis acid and Lewis base, we investigated the formation of encounter complexes in two amine–borane FLP systems experimentally. In case of

1127

Synlett   F. Holtrop et al.   THIEME OPEN ACCESS   Cluster

$N(3,5-tBu_2C_6H_3)_3/B(3,5-(CF_3)_2C_6H_3)_3$ it was shown that photoinduced SET can be generally observed in FLPs with matching electron affinities and ionization potentials. For the $N(3,5-tBu_2C_6H_3)_3/B(3,5-tBu_2C_6H_3)_3$ FLP system a cocrystal containing both components was obtained, which showed positional disorder of the B and N centers due to random arrangement of the individual components in the crystal. This moreover showed the potential for homodimer formation in dispersion interaction-governed systems. This work represents an important contribution to the structural characterization of an intermolecular FLP and the structural verification of the concept of the encounter complex in FLP chemistry. Future investigations will focus on the use of dissimilar Lewis acids and Lewis bases to favor heterofragment interactions and ultimately allow the unambiguous identification of an encounter complex in the crystalline state.

Conflict of Interest

The authors declare no conflict of interest.

Funding Information

Acknowledgment

Supporting Information

Supporting information for this article is available online at https://doi.org/10.1055/a-1928-4902.

References and Notes

(1) Welch, G. C.; Juan, R. R. S.; Masuda, J. D.; Stephan, D. W. *Science* **2006**, *314*, 1124.

(2) (a) Stephan, D. W.; Erker, G. *Angew. Chem. Int. Ed.* **2010**, *49*, 46. (b) Stephan, D. W. *Acc. Chem. Res.* **2015**, *48*, 306. (c) Stephan, D. W. *J. Am. Chem. Soc.* **2015**, *137*, 10018. (d) Stephan, D. W. *Science* **2016**, *354*, aaf7229. (e) Paradies, J. *Coord. Chem. Rev.* **2019**, *380*, 170. (f) Jupp, A. R.; Stephan, D. W. *Trends Chem.* **2019**, *1*, 35.

(3) (a) Paradies, J. *Eur. J. Inorg. Chem.* **2019**, 283. (b) Jupp, A. R. *Dalton Trans.* **2022**, *51*, 10681.

(4) (a) Rokob, T. A.; Hamza, A.; Stirling, A.; Soós, T.; Pápai, I. *Angew. Chem. Int. Ed.* **2008**, *47*, 2435. (b) Bistoni, G.; Auer, A. A.; Neese, F. *Chem. Eur. J.* **2017**, *23*, 865. (c) Grimme, S.; Kruse, H.; Goerigk, L.; Erker, G. *Angew. Chem. Int. Ed.* **2010**, *49*, 1402. (d) Skara, G.; Pinter, B.; Top, J.; Geerlings, P.; De Proft, F.; De Vleeschouwer, F. *Chem. Eur. J.* **2015**, *21*, 5510. (e) Zeonjuk, L. L.; Vankova, N.; Mavrandonakis, A.; Heine, T.; Röschenthaler, G. V.; Eicher, J. *Chem. Eur. J.* **2013**, *19*, 17413.

(5) Rocchigiani, L.; Ciancaleoni, G.; Zuccaccia, C.; Macchioni, A. *J. Am. Chem. Soc.* **2014**, *136*, 112.

(6) Holtrop, F.; Jupp, A. R.; van Leest, N. P.; Paradiz Dominguez, M.; Williams, R. M.; Brouwer, A. M.; de Bruin, B.; Ehlers, A. W.; Slootweg, J. C. *Chem. Eur. J.* **2020**, *26*, 9005.

(7) A π–π-stacked co-crystal of 1-Br-4-$(NMe_2)C_6H_4$ and $B(C_6F_5)_3$ was reported: Aramaki, Y.; Imaizumi, N.; Hatta, M.; Kumagai, J.; Ooi, T. *Chem. Sci.* **2020**, *11*, 4305.

(8) (a) Rösel, S.; Balestrieri, C.; Schreiner, P. R. *Chem. Sci.* **2017**, *8*, 405. (b) Rösel, S.; Becker, J.; Allen, W. D.; Schreiner, P. R. *J. Am. Chem. Soc.* **2018**, *140*, 14421.

(9) Holtrop, F.; Jupp, A. R.; Kooij, B. J.; van Leest, N. P.; de Bruin, B.; Slootweg, J. C. *Angew. Chem. Int. Ed.* **2020**, *59*, 22210.

(10) Geier, S. J.; Stephan, D. W. *J. Am. Chem. Soc.* **2009**, *131*, 3476.

(11) (a) Pollice, R.; Bot, M.; Kobylianskii, I. J.; Shenderovich, I.; Chen, P. *J. Am. Chem. Soc.* **2017**, *139*, 13126. (b) Schümann, J. M.; Wagner, J. P.; Eckhardt, A. K.; Quanz, H.; Schreiner, P. R. *J. Am. Chem. Soc.* **2021**, *143*, 41.

(12) The syntheses of all-*meta*-Ph-substituted triarylamine and triarylborane were attempted. However, only in common organic solvents insoluble products were obtained precluding purification, characterization, and further investigations.

(13) Bedford, R. B.; Betham, M. *Tetrahedron Lett.* **2007**, *48*, 8947.

(14) Kahr, B.; Van Engen, D.; Gopalan, P. *Chem. Mater.* **1993**, *5*, 729.

(15) Kolychev, E. L.; Bannenberg, T.; Freytag, M.; Daniliuc, C. G.; Jones, P. G.; Tamm, M. *Chem. Eur. J.* **2012**, *18*, 16938.

(16) Borger, J. E.; Ehlers, A. W.; Lutz, M.; Slootweg, J. C.; Lammertsma, K. *Angew. Chem. Int. Ed.* **2015**, *55*, 613.

(17) Osi, A.; Mahaut, D.; Tumanov, N.; Fusaro, L.; Wouters, J.; Champagne, B.; Chardon, A.; Berionni, G. *Angew. Chem. Int. Ed.* **2202**, *61*, e202112342.

(18) **Synthesis of $B(3,5-tBu_2C_6H_3)_3$**
$[Me_3NH]Cl$ (50 mg, 0.55 mmol) was added to a solution of $Na[B(3,5-tBu_2C_6H_3)_4]$ (396 mg, 0.5 mmol) in MeCN (10 mL) at ambient temperature. The white suspension was stirred for 3 h and subsequently filtered over Celite. Volatiles were removed from the filtrate in vacuo. The resulting white solid was dissolved in THF (40 mL), and 2,2,6,6-tetramethylpiperidine (78 mg, 0.55 mmol, 0.093 mL) was added at ambient temperature. The mixture was stirred for 1 h, after which volatiles were removed in vacuo. The residue was extracted into diethyl ether (30 mL), and the filtrate was concentrated until incipient crystallization and stored at –30 °C to yield colorless analytically pure crystals of $B(3,5-tBu_2C_6H_3)_3$. Yield: 260 mg (0.45 mmol, 90%); mp 255 °C. HRMS (LIFDI): m/z calcd for $C_{42}H_{63}B$: 578.5030; found: 578.5028. IR (neat): v = 2952, 2902, 2866, 1584, 1475, 1460, 1412, 1390, 1361, 1309, 1247, 1220, 993, 895, 885, 822, 725, 671, 539 cm^{-1}. ^{1}H NMR (500 MHz, CDCl$_3$): δ = 7.60 (s, 3 H, *p-CH*), 7.51 (s, 6 H, *o-CH*), 1.35 (s, 54 H, *t*Bu). ^{13}C{^{1}H} NMR (125.6 MHz, CDCl$_3$): δ = 148.9 (*m-C$_6$H$_3$t*Bu$_2$), 133.7 (*o-C$_6$H$_3$t*Bu$_2$), 125.0 (*p-C$_6$H$_3$t*Bu$_2$), 35.0 ($C(CH_3)_3$), 31.8 ($C(CH_3)_3$) (*ipso-C$_6$H$_3$t*Bu$_2$ not observed). ^{11}B NMR (160.5 MHz, CD$_3$CN): δ = 68.4 (very br).

(19) Sreenath, K.; Suneesh, C. V.; Gopidas, K. R.; Flowers, R. A. II. *J. Phys. Chem. A* **2009**, *113*, 6477.

1128

Synlett   F. Holtrop et al.   THIEME OPEN ACCESS   Cluster

(20) Zheng, X.; Wang, X.; Qiu, Y.; Li, Y.; Zhou, C.; Sui, Y.; Li, Y.; Ma, J.; Wang, X. *J. Am. Chem. Soc.* **2013**, *135*, 14912.

(21) Lawrence, E. J.; Oganesyan, V. S.; Wildgoose, G. G.; Aschley, A. E. *Dalton Trans.* **2013**, *42*, 782.

(22) Welch, G. C.; Stephan, D. W. *J. Am. Chem. Soc.* **2007**, *129*, 1880.

(23) **Synthesis of N(3,5-*t*Bu$_2$C$_6$H$_3$)$_3$/B(3,5-*t*Bu$_2$C$_6$H$_3$)$_3$**
N(3,5-*t*Bu$_2$C$_6$H$_3$)$_3$ (10 mg, 0.017 mmol) and B(3,5-*t*Bu$_2$C$_6$H$_3$)$_3$ (10 mg, 0.017 mmol) were dissolved in toluene-d_8 (0.5 mL). Storage

of the solution at –30 °C overnight afforded colorless crystals of N(3,5-*t*Bu$_2$C$_6$H$_3$)$_3$/B(3,5-*t*Bu$_2$C$_6$H$_3$)$_3$. Yield: 16 mg (0.014 mmol, 80%); mp 224 °C. IR (neat): ν = 2951, 2902, 2866, 1582, 1495, 1476, 1461, 1447, 1426, 1413, 1391, 1361, 1307, 1246, 1221, 1204, 1130, 1038, 1008, 993, 924, 896, 886, 865, 822, 727, 720, 711, 694, 671, 539, 463 cm^{-1}. ^{1}H NMR (500 MHz, C$_6$D$_6$): δ 8.03 (s, 3 H, p-CH), 7.86 (s, 6 H, o-CH), 7.46 (s, 3 H, p-CH), 7.27 (s, 6 H, o-CH), 1.32 (s, 54 H, *t*Bu), 1.23 (s, 54 H, *t*Bu).